

## Are We Close to an Equilibrated Quark-Gluon Plasma? Nonequilibrium Analysis of Particle Production in Ultrarelativistic Heavy Ion Collisions

S. A. Bass, M. Belkacem, M. Brandstetter, M. Bleicher, L. Gerland, J. Konopka, L. Neise,  
C. Spieles, S. Soff, H. Weber, H. Stöcker, and W. Greiner

*Institut für Theoretische Physik, Johann Wolfgang Goethe Universität,  
Robert Mayer Strasse 8-10, D-60054 Frankfurt am Main, Germany*

(Received 19 November 1997)

Ratios of hadronic abundances are analyzed for  $pp$  and nucleus-nucleus collisions at  $\sqrt{s} \approx 20$  GeV using the microscopic ultrarelativistic quantum molecular dynamics transport model. Secondary interactions significantly change the primordial hadronic composition of the system. A strong dependence on rapidity is predicted. Without assuming thermal and chemical equilibrium, predicted hadron yields and ratios agree with many of the data ( $\pi/p$ ,  $d/p$ ,  $\bar{p}/p$ ,  $\bar{\Lambda}/\Lambda$ ,  $\bar{\Xi}/\bar{\Lambda}$ , etc.). [S0031-9007(98)07647-9]

PACS numbers: 25.75.Dw, 12.38.Mh, 24.10.Lx, 24.85.+p

Hadron abundances and ratios have been suggested as possible signatures for exotic states and phase transitions in dense nuclear matter. In addition they have been applied to study the degree of chemical equilibration in a relativistic heavy-ion reaction. Bulk properties like temperatures, entropies, and chemical potentials of highly excited hadronic matter have been extracted assuming thermal and chemical equilibrium [1–7].

The present Letter confronts the conclusions of a series of publications which have attempted to fit the available data obtained at the BNL Alternating Gradient Synchrotron [8] and at the CERN Super Proton Synchrotron (SPS) [9] on hadron yields and ratios. The latter have been done either in the framework of a hadronizing quark-gluon plasma (QGP) droplet [7,10] or of a hadron gas in thermal and chemical equilibrium [6] (including elementary  $p + p$  interactions [11]). It has been shown that the thermodynamic parameters  $T$  and  $\mu_B$  imply that these systems have been either very close to or even above the critical  $T$ ,  $\mu_B$  line for QGP formation [6,7].

Here, in contrast, the nonequilibrium microscopic ultrarelativistic quantum molecular dynamics transport model (UrQMD) [12,13] is used to calculate hadron ratios without thermalization assumptions. We tackle the following questions.

(1) Is this microscopic model able to describe hadron production (including yields and ratios)?

(2) To what extent do the hadron ratios depend on rapidity? How strong is their sensitivity to experimental acceptance cuts?

(3) Do isospin and secondary interactions (rescattering) play a major role or is the hadronic makeup of the system fixed after the first primordial highly energetic nucleon-nucleon collisions?

For our analysis we employ the ultrarelativistic quantum molecular dynamics model [12,13] which is based on analogous principles as the (relativistic) quantum molecular dynamics model [14–16]. The UrQMD model is ideally suited to study questions involving hadrochem-

istry—its collision term treats 55 different isospin ( $T$ ) degenerate baryon ( $B$ ) species (including nucleon, delta, and hyperon resonances with masses up to 2 GeV) and 32 different  $T$ -degenerate meson ( $M$ ) species, including (strange) meson resonances as well as the corresponding antiparticles. A detailed overview of the model, including the elementary cross sections and string excitation scheme, as well as an in-depth analysis of particle production and freeze-out, has been published in [12,13].

The first question remains as follows: Is a microscopic transport model able to describe hadron production yields and ratios? Hadron production in elementary high energy proton-proton or nucleon-nucleon reactions is modeled in UrQMD via a string excitation scheme. The parameters are chosen such to yield the best possible agreement with available data (for a compilation of available  $p + p$  data, we refer to [11]). In most cases the fit yields good agreement to hadron yields and momentum distributions. Notable exceptions are the  $\phi$  production which is underestimated by a factor of 2.  $\Lambda + \Sigma^0$  as well as the  $\bar{\Lambda} + \bar{\Sigma}^0$  production are overestimated by  $>50\%$ . Problems in the strangeness sector are common to most string models and indicate that strangeness production is not yet fully understood on the elementary level [17].

Figure 1 compares the UrQMD hadron ratios with experimental measurements [9]. We use a data compilation which has been published in Ref. [6]. The open circles represent the measurements whereas the full circles show the respective UrQMD calculation for S + Au at 200 GeV/nucleon and impact parameters between 0 and 1.5 fm. For each ratio, the respective acceptance cuts, as listed in [6], have been applied. The crosses denote a fit with a dynamical hadronization scheme, where thermodynamic equilibrium between a quark blob and the hadron layer is imposed [7]. A good overall agreement between the data and UrQMD is observed, similar in quality to that of the hadronization model. Large differences, however, are visible in the  $\phi/(\rho + \omega)$ ,  $K_S^0/\Lambda$ , and  $\Omega/\Xi$  ratios. Those discrepancies can be traced back to the elementary

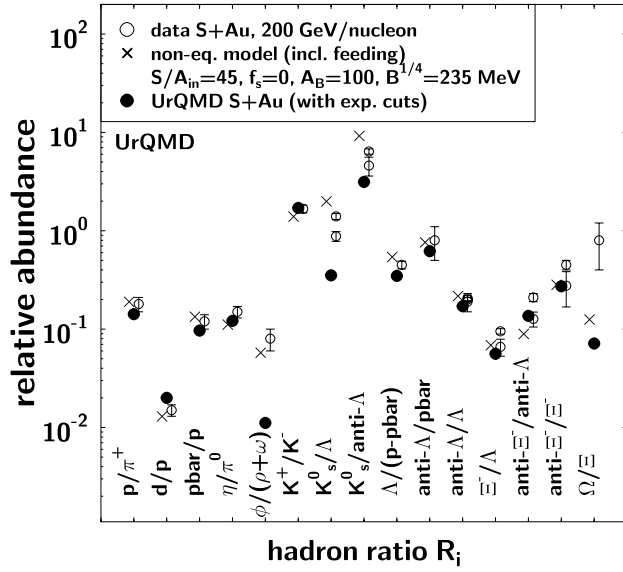


FIG. 1. Comparison between the UrQMD model (full circles) and data (open circles) for the system S + Au(W,Pb) at 200 GeV/nucleon. Also shown is a fit by a microscopic hadronization model (crosses). Both nonequilibrium models agree well with the data. Discrepancies are visible for the  $\phi/(\rho + \omega)$ ,  $K_S^0/\Lambda$ , and  $\Omega/\Xi$  ratios.

UrQMD input, e.g., the underestimation of the  $\phi$ -meson yield.

A thermal and chemical equilibrium model can be even used to fit the hadron ratios of the UrQMD calculation displayed in Fig. 1. The parameters of the thermal model fit to the microscopic calculation in the  $y_{lab} = 3 \pm 0.5$  region yields a temperature of  $T = 145$  MeV and a baryochemical potential of  $\mu_B = 165$  MeV. However, the assumption of global thermal and chemical equilibrium is not justified: Both the discovery of directed collective flow of baryons and antiflow of mesons in Pb + Pb reactions at 160 GeV/nucleon energies [18] as well as transport model analysis, which show distinctly different freeze-out times and radii for different hadron species [12,19], indicate that the yields and ratios result from a complex nonequilibrium time evolution of the hadronic system (see Fig. 4 below). A thermal model fit to a nonequilibrium transport model (and to the data) may therefore not seem meaningful.

To what extent do the hadron ratios depend on rapidity and transverse momentum? How strong is their sensitivity to experimental acceptance cuts? The rapidity dependence of individual hadron ratios  $R_i$  is shown in Fig. 2: The  $p/\pi^+$ ,  $\eta/\pi^0$ ,  $K^+/K^-$ ,  $\bar{p}/p$ ,  $\Lambda/p$ , and  $K_S^0/\Lambda$  ratios are plotted as a function of  $y_{lab}$ . A strong dependence of the ratios  $R_i$  on the rapidity is visible—some ratios, especially those involving (anti)-baryons, change by orders of magnitude when going from target rapidity to midrapidity. The  $y$  dependence is enhanced by the heavy target which leads to strong absorption of mesons and antibaryons. The observed shapes of  $R_i(y)$  are distinctly different from a fireball ansatz incorporating additional longitudinal flow:

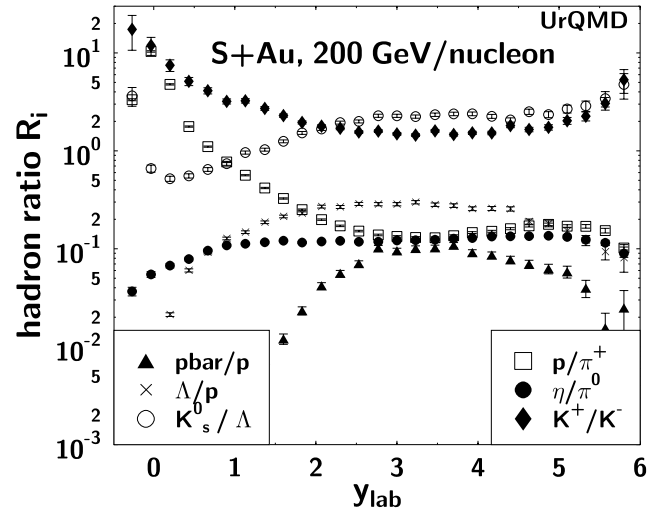


FIG. 2. Rapidity dependence of hadron ratios in the UrQMD model for the system S + Au(W,Pb) at CERN/SPS energies. The ratios vary by orders of magnitude, yielding different  $T$  and  $\mu_B$  values for different rapidity intervals.

There, the ratios would also be symmetric with respect to the rapidity of the central source. When fitting a thermal model to data, one must take this rapidity dependence into account and correct for different experimental acceptances.

The strong rapidity dependence also indicates clearly a strong dependence of the hadron ratios on the experimental acceptances. Imposing additional cuts on  $p_t$  may drastically change yields and ratios (e.g., in the case of the  $K_0/\bar{\Lambda}$  ratio, the additional cut on the  $p_t$  of the kaons in the experiment causes a decrease of the ratio by almost 1 order of magnitude).

Do isospin and secondary interactions play a major role or is the hadronic makeup of the system fixed after the first primordial highly energetic nucleon-nucleon collisions? Since even the particle abundances in elementary proton-proton reactions may be described in a thermal model [11], one could speculate that the hadronic final state of a nucleus-nucleus collision should not differ considerably from the primordial “thermal” composition.

Figure 3 shows the UrQMD prediction for the heavy system Pb + Pb. The ratios around midrapidity (full circles) are compared to those stemming from elementary proton-proton reactions (open squares) and those from an isospin-weighted nucleon-nucleon calculation (open triangles), which is obtained by weighting a cocktail of  $pp$ ,  $pn$ , and  $nn$  events such that the proton and neutron numbers in the Pb nuclei are properly taken into account (i.e., a first collision ansatz):  $NN(\text{Pb} + \text{Pb}) = 0.155(pp) + 0.478(pn) + 0.367(nn)$ .

The correct isospin treatment is of utmost importance, as it has a large influence on the primordial hadron ratios. Because of isospin conservation, the  $\bar{p}/p$  and  $\Lambda/(p - \bar{p})$  ratios are enhanced by  $\sim 30\%$  and  $\sim 35\%$ , respectively, since it is easier to produce neutral or negatively charged particles in a  $nn$  or  $pn$  collision than in a  $pp$  interaction.

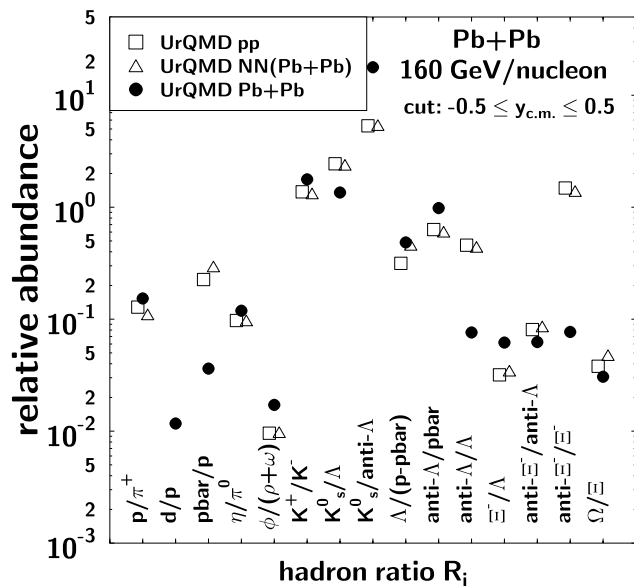


FIG. 3. UrQMD prediction for hadron ratios in Pb + Pb collisions at midrapidity (full circles). The ratios are compared to a superposition of  $pp$ ,  $pn$ , and  $nn$  reactions with the isospin weight of the Pb + Pb system (open triangles), i.e., a first collision approach.

In a heavy system such as Pb + Pb, rescattering effects are even larger than those accounted for by isospin conservation. Because of the large number of baryons around midrapidity, antibaryon annihilation at midrapidity occurs frequently and therefore ratios involving antibaryons are strongly suppressed. Most prominent examples are the  $\bar{\Xi}/\Xi$  (a factor of 20 suppression),  $\bar{p}/p$  (a factor of 8 suppression), and the  $K_S^0/\bar{\Lambda}$  (a factor of 3 enhancement) ratios. The  $\phi/(\rho + \omega)$  yield is enhanced by a factor of 2. Here, the  $\phi$  enhancement via  $K^+K^-$  scattering evidently outweighs the  $\rho$  enhancement via  $\pi^+\pi^-$  scattering. *Strangeness enhancement* is therefore also present in a hadronic transport approach and does not necessarily point towards the formation of a QGP (as predicted, e.g., in Ref. [3]). A thermal model fit at midrapidity yields values of  $T = 140$  MeV and  $\mu_B = 210$  MeV.

How do the ratios evolve from their primordial value (fixed in the first high energy nucleon-nucleon reactions) to the final values and which processes dominate their evolution? The upper frame of Fig. 4 shows the time evolution of the  $p/\pi^+$ ,  $\bar{p}/p$ ,  $\Lambda/(p - \bar{p})$ , and  $\bar{\Lambda}/\Lambda$  ratios at midrapidity for Pb + Pb. As is to be expected, the initial ratios are identical to the values given by the isospin-weighted nucleon-nucleon calculation. The hot and dense reaction phase lasts only until approximately 10 fm/c; thereafter the system rapidly expands. No early saturation of the ratios in the hot and dense reaction phase is observed, indicating that the system does not reach the final ratios in that early phase. During the hot and dense phase, the  $p/\pi^+$  ratio drops almost by a factor of 3 due to massive pion production and excitation of protons into

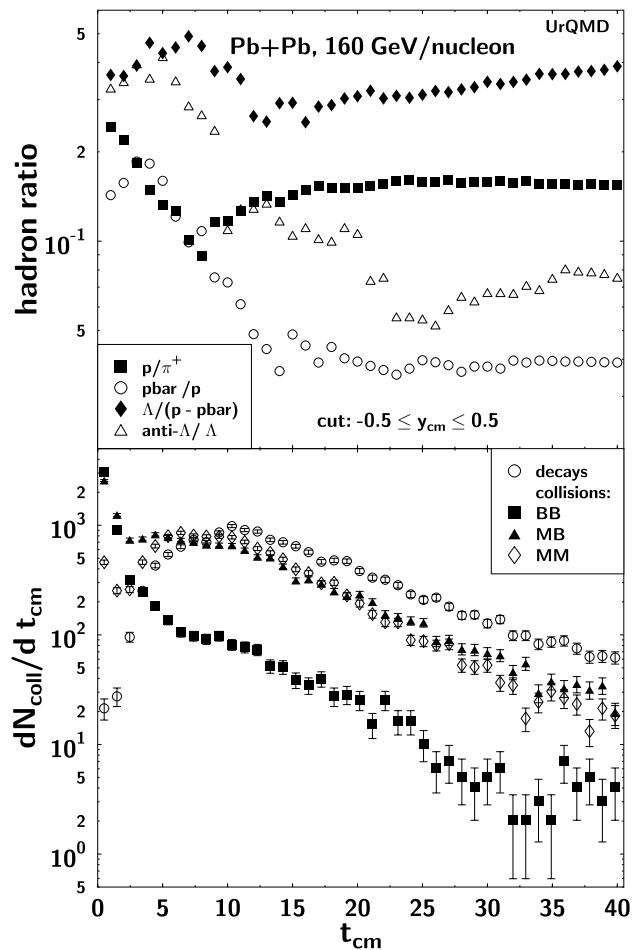


FIG. 4. Top: Time evolution of the  $p/\pi^+$ ,  $\bar{p}/p$ ,  $\Lambda/(p - \bar{p})$ , and  $\bar{\Lambda}/\Lambda$  ratios at midrapidity for Pb + Pb. At  $t = 40$  fm/c—at which kinetic freeze-out has occurred for 95% of the mesons and 75% of the baryons—the  $\Lambda/(p - \bar{p})$  and  $\bar{\Lambda}/\Lambda$  ratios have not yet saturated. Bottom: Collision and decay rates. Baryon-baryon interactions dominate the early reaction stage, subsequently the system is driven by meson-baryon and meson-meson interactions and the late reaction stages are dominated by decays of resonant states.

resonant states, but then increases again by a factor of 2 during the later reaction stages when resonance decays again populate the proton states. Saturation occurs close to  $t = 30$  fm/c (close to the kinetic freeze-out for pions). The  $\bar{p}/p$  ratio drops due to massive  $B\bar{B}$  annihilation by a factor of 8. Similarly, the  $\bar{\Lambda}/\Lambda$  drops also by a factor of 10. Both the  $\bar{p}/p$  and the  $\bar{\Lambda}/\Lambda$  show an initial increase due to the enhanced production of antibaryons through multistep excitation processes in the early, dense reaction stage [20], which is subsequently countered by massive  $B\bar{B}$  annihilation.

The kinetic freeze-out of the system does not occur at one particular time, but each particle species exhibits its own, broad, freeze-out distribution in space-time [12,19]: at  $t = 40$  fm/c, 95% of the mesons and approximately 75% of the baryons have frozen out [12]. Thus, this

time provides us with a rather conservative estimate on the saturation time of the system. However, even at  $t = 40$  fm/c, the  $\Lambda/(p - \bar{p})$  and  $\bar{\Lambda}/\Lambda$  ratios have not yet saturated.

The lower frame of Fig. 4 shows the time dependence of the collision and decay rates for the Pb + Pb reaction. The system is initially driven by primordial baryon-baryon ( $BB$ ) reactions, the intermediate reaction stages are dominated by both, meson-baryon ( $MB$ ) and meson-meson ( $MM$ ) collisions, giving, in the late reaction stages, way to decays of meson- and baryon resonances. Both  $MB$  and  $MM$  rescattering change the absolute yields and ratios drastically, e.g., the  $K^+$  multiplicity at midrapidity rises from initially 12.5 to a final value of 34 and the  $\Lambda + \Sigma^0$  multiplicity rises from 5 to 16. The decays of excited hadrons feed the final hadronic composition of the system; i.e., 80% of the final pions result from late resonance decays and only 20% originated from string fragmentations. The dominant pion sources among the resonances are the  $\rho$ ,  $\Delta(1232)$ ,  $\omega$ , and  $K^*$  resonances (ordered according to their relative importance) which together account for 80% of the pions stemming from decays.

The treatment of the  $B\bar{B}$  annihilation cross section influences the final yield of  $\bar{p}$ 's and  $\bar{Y}$ 's: If  $\sigma_{\text{ann}}^{pp}(\sqrt{s})$  is used for all  $B\bar{B}$  annihilations, instead of rescaling the cross section to equivalent relative momenta, the  $\Xi$  yield in Pb + Pb is enhanced by a factor of 3. The  $\bar{p}$  and  $\bar{Y}$  yields are enhanced by 50% and 25%, respectively. A systematic study of the different  $B/\bar{B}$  ratios, as functions of system size, impact parameter, transverse momentum, and azimuthal angle, is needed to fix experimentally the  $\bar{Y}B$  and the  $\bar{Y}Y$  annihilation cross sections [21].

In summary, hadronic abundances for  $\sqrt{s_{NN}} \sim 20$  GeV from a microscopic transport model agree well with data. A comparison with a first collision ansatz shows a large influence of secondary interactions. The early reaction stage is dominated by  $BB$  reactions.  $MB$  and  $MM$  rescattering subsequently change the ratios and yields by factors of 2–3 and  $B\bar{B}$  annihilation reduces  $\bar{B}$  and  $\bar{Y}$  ratios by a factor of 10. Feeding from excited resonant states finally changes the ratios again by 50%.

The present results show that the nonequilibrium kinetic theory gives a reasonable description of hadron ratio data without invoking the formation of a QGP. The predicted complex rapidity dependence of the hadron ratios can help to distinguish such models from equilibrium QGP scenarios at CERN/SPS energies.

This work was supported by GSI, BMBF, Graduiertenkolleg "Theoretische und experimentelle Schwerionenphysik" and DFG.

[1] H. Stöcker, W. Greiner, and W. Scheid, Z. Phys. A **286**, 121 (1978); D. Hahn and H. Stöcker, Nucl. Phys. A**476**,

- 718 (1988); A**452**, 723 (1986); H. Stöcker and W. Greiner, Phys. Rep. **137**, 277 (1986).
- [2] R. Stock, Phys. Rep. **135**, 261 (1986).
- [3] J. Rafelski and B. Müller, Phys. Rev. Lett. **48**, 1066 (1982); J. Rafelski, Phys. Rep. **88**, 331 (1982); P. Koch, B. Müller, and J. Rafelski, Phys. Rep. **142**, 167 (1986).
- [4] J. Letessier, A. Tounsi, U. Heinz, J. Sollfrank, and J. Rafelski, Phys. Rev. Lett. **70**, 3530 (1993); J. Letessier, J. Rafelski, and A. Tounsi, Phys. Lett. B **321**, 394 (1994); J. Rafelski and M. Danos, Phys. Rev. C **50**, 1684 (1994); J. Sollfrank, M. Gadzicki, U. Heinz, and J. Rafelski, Z. Phys. C **61**, 659 (1994).
- [5] J. Cleymans, M.I. Gorenstein, J. Stalnacke, and E. Suhonen, Phys. Scr. **48**, 277 (1993); J. Cleymans and H. Satz, Z. Phys. C **57**, 135 (1993); J. Cleymans, D. Elliott, H. Satz, and R.L. Thews, Z. Phys. C **74**, 319 (1997).
- [6] P. Braun-Munzinger, J. Stachel, J.P. Wessels, and N. Xu, Phys. Lett. B **344**, 43 (1995); **365**, 1 (1996); P. Braun-Munzinger and J. Stachel, Nucl. Phys. A**606**, 320 (1996).
- [7] C. Spieles, H. Stöcker, and C. Greiner, Eur. Phys. J. C **2**, 351 (1998); C. Greiner and H. Stöcker, Phys. Rev. D **44**, 3517 (1991).
- [8] S.E. Eiseman *et al.*, Phys. Lett. B **297**, 44 (1992); J. Barrette *et al.*, Z. Phys. C **59**, 211 (1993); T. Abbott *et al.*, Phys. Rev. C **50**, 1024 (1994); G.S.F. Stephans *et al.*, Nucl. Phys. A**566**, 269c (1994); S.E. Eiseman *et al.*, Phys. Lett. B **325**, 322 (1994); J. Barrette *et al.*, Phys. Lett. B **351**, 93 (1995).
- [9] E. Andersen *et al.*, Phys. Lett. B **294**, 127 (1992); **327**, 433 (1994); M. Murray *et al.*, Nucl. Phys. A**566**, 589c (1994); J.T. Mitchell, Nucl. Phys. A**566**, 415c (1994); M. Gadzicki *et al.*, Nucl. Phys. A**590**, 197c (1995); S. Abatzis *et al.*, Phys. Lett. B **316**, 615 (1993); D.D. Bari *et al.*, Nucl. Phys. A**590**, 307c (1995).
- [10] H.W. Barz, B.L. Friman, J. Knoll, and H. Schultz, Nucl. Phys. A**484**, 661 (1988).
- [11] F. Becattini and U. Heinz, Z. Phys. C **76**, 269 (1997).
- [12] S.A. Bass, M. Belkacem, M. Bleicher, M. Brandstetter, L. Bravina, C. Ernst, L. Gerland, M. Hofmann, S. Hofmann, J. Konopka, G. Mao, L. Neise, S. Soff, C. Spieles, H. Weber, L.A. Winkelmann, H. Stöcker, W. Greiner, C. Hartnack, J. Aichelin, and N. Amelin, Prog. Part. Nucl. Phys. **41**, 225 (1998); nucl-th/9803035.
- [13] M. Bleicher, S.A. Bass, M. Belkacem, M. Brandstetter, L. Bravina, C. Ernst, L. Gerland, M. Hofmann, S. Hofmann, G. Mao, L. Neise, S. Soff, C. Spieles, H. Weber, H. Stöcker, and W. Greiner (to be published).
- [14] G. Peilert, A. Rosenhauer, H. Stöcker, W. Greiner, and J. Aichelin, Mod. Phys. Lett. A **3**, 459 (1988).
- [15] J. Aichelin, Phys. Rep. **202**, 233 (1991).
- [16] H. Sorge, H. Stöcker, and W. Greiner, Ann. Phys. (N.Y.) **192**, 266 (1989).
- [17] V. Topor Pop *et al.*, Phys. Rev. C **52**, 1618 (1995).
- [18] S. Nishimura *et al.*, Nucl. Phys. A**638**, 459 (1998); H. Appelshäuser *et al.*, Phys. Rev. Lett. **80**, 4136 (1998).
- [19] H. Sorge, Phys. Rev. Lett. **78**, 2309 (1997).
- [20] A. Jahns, H. Stöcker, W. Greiner, and H. Sorge, Phys. Rev. Lett. **68**, 2895 (1992).
- [21] A. Jahns, C. Spieles, H. Sorge, H. Stöcker, and W. Greiner, Phys. Rev. Lett. **72**, 3464 (1994).